EAST EUROPEAN JOURNAL OF PHYSICS. **3.** 209-222 (2025)
DOI:10.26565/2312-4334-2025-3-18 ISSN 2312-4334

EFFECTS OF NATURAL CONVECTION AND RADIATION ON MHD STAGNATION POINT NANO-FLUID FLOW PAST A STRETCHABLE SURFACE WITH VELOCITY SLIP AND NEWTONIAN HEATING

G.P. Gifty[a], S.B. Padhi[a], B.K. Mahatha[b], G.K. Mahato[c]*
[a]*Department of Mathematics, Centurion University of Technology and Management, Odisha, India*
[b]*Rajkiyakrit +2 High School, Latbedhwa, Koderma, Jharkhand, India*
[c]*Department of Mathematics, Amity Institute of Applied Sciences, Amity University Jharkhand, Ranchi-835303, India*
**Corresponding author E-mail: mahatogk@gmail.com*
Received June 6, 2025; revised August 7, 2025; accepted August 11, 2025

MHD stagnation point natural convection flow of a viscous, incompressible, electrically conducting, and heat radiating nanofluid past a stretchy surface with velocity slip and Newtonian heating in the presence of a transverse magnetic field is examined. Governing nonlinear partial differential equations are solved with the help of Matlab's bvp4c technique. To confirm robustness and accuracy of the result, the numerical findings in this study are compared with the existing literature, and they are found to be in good agreement. Effects of various parameters on velocity, temperature, and species concentration are computed and presented in the form of graphs whereas the effects on skin friction, the heat transfer rate and mass transfer rate are tabulated. As a result of enhanced thermal energy accumulation or diffusion, nanofluid temperature is increased by Brownian motion, thermophoretic diffusion, velocity slip, convective heating, nonlinear thermal radiation, and Prandtl number. Rate of heat transfer is getting enhanced by temperature ratio, convective heating, and thermal Grashof number due to increased thermal gradients and buoyancy-driven heat transport. Such nanofluid flows have the potential to be used in a number of heat transfer processes such as renewable energy devices including MHD power generators, etc.
Keywords: *MHD, Nano-Fluid, Natural Convection, Radiation, Velocity Slip, Newtonian Heating*
PACS: 47.11.-j, 47.10.ab, 02.30.Jr

INTRODUCTION

Magnetohydrodynmics deals with the study of the dynamic flow of the fluids that conduct electricity. It connects the fluid dynamics and the electromagnetism. It has various applications especially in the field of marine propulsion, astrophysical simulations, forcasting of the space weather etc., Nandini *et al*. [1] made an analysis of the effects of non-linear radiation in a Darcy-forccheimer model in a rotating channel. The parameters of rotation, magnetic, stretching ratio, Reynolds number, and fluid velocity are all inversely related. In contrast to the parameters of rotation and magnetic field, the Nusselt parameter is correlated with Reynolds number. The fluid temperature is inversely correlated with Reynolds number and similar to rotation and magnetic field. The Reynolds number and magnetic field have a comparable relationship with skin friction. Ouyang *et al*. [2] found that in contrast to the dihybrid nanofluid, they discovered that the trihybrid nanofluid responded favorably to every parameter. Hasana *et al*. [3] taking the radiative heat flux and exothermic chemical reactions found that the Rayleigh number and the nanofluid's velocity are directly correlated. While it is in opposition to thermal radiation, the Frank-Kemenetskii number is proportional to fluid velocity. It is found that the Rayleigh number's critical value is 3×10^4. Heat transfer is at its highest when the nanoparticle's volume fraction is 3%. Shilpa *et al*. [4] took the Carreauternary hybrid nano fluid for their study on Artificial neural network to find the rate of heat and mass transfer in MHD flow across a vertical cylinder. They discovered that the rate at which heat was transported was significantly higher when they substituted ternary nanoparticles for standard nanoparticles. Accelerated Schimdt number and chemical reaction parameters exacerbate the rate of mass transfer in nanofluids. Additionally, these characteristics raise the fluid's concentration. Khan *et al*. [5] considering the radiating couple stress on the MHD nanofluid flow, discovered that, in contrast to fractional parameters, velocity is proportional to Grashof number, couple stress, and thermal variables. Skin friction varies similarly in response to pressure gradients. The Nusselt number appears to increase exponentially in relation to the Reynolds and Eckert numbers. As the fractional parameter grows, the Bejan number rises as well. Vaidya *et al*. [6] considering gold nanoparticles for thermal radiation in cancer treatment process in flow of Phan-Thien-Tanner MHD found that the fluid flow is enhanced by the Weissenberg number and magnetic parameter, but it is inhibited by the Hall parameter. The fluid's temperature is directly correlated with the thermal radiation parameter. The Weissenberg number and shear stress are connected. Fatunmbi *et al*. [7] considering micropolar water-based iron oxide and silver nanoparticles in the fluid found that when on increasing the suction/injection and magnetic parameters results in a significant decrease in fluid flow. When the heat generation parameter is raised, the fluid's temperature rises; conversely, when the heat exponent is raised, the opposite occurs. Heat transmission in the nanofluid is accelerated by radiation. Saranya *et al*. [8] found that when two disks are rotated the rate of flow is enhanced. They discovered that raising the Reynolds number improved micro rotation. The fluid's temperature is directly correlated with its Reynolds

Cite as: G.P. Gifty, S.B. Padhi, B.K. Mahatha, G.K. Mahato, East Eur. J. Phys. 3, 209 (2025), https://doi.org/10.26565/2312-4334-2025-3-18

number and thermal radiation. When vortex viscosity and magnetic field act on the fluid, fluid velocity decreases; conversely, when the volume fraction of the nanoparticle increases, the opposite occurs. Iqbal *et al*. [9] made a study taking microorganisms and the bioconvective flow into consideration. As the thermophoretic effect increases, the temperature rises. The Nusselt number rises in tandem with the Prandtl number. The fluid's velocity and its Forchheimer number are inversely correlated. When the fluid's temperature is raised, radiation raises it. The Pecelt number has an inverse relationship with the fluid's concentration. Alqurashi *et al*. [10] using chemical engineering applications in mixed convection mode, made a detailed study and found that the fluid's velocity is correlated with the mixed convection coefficient and in opposition to the Darcy number and relaxation time coefficient. When the Eckert number and radiation are increased, the temperature rises. The fluid's concentration rises as the thermophoresis parameter rises, but the opposite is true for the Lewis number and chemical reaction coefficient.

Nanofluid is obtained by dispersing nanoparticles like copper, gold, silver etc., in base fluids like water, glycol etc., these nanofluid enhance the thermal properties by increasing the rate of heat and mass transfer. It is mostly used as a coolant in various industries like nuclear reactors, electronic coolings, solar energy, aerospace engineering, etc., Afifi *et al*. [11] studied effects of FEM and AGM in the convection mode in the fluid flow. When the relaxation to retardation ratio rises, the temperature always rises; however, when the Prandtl number falls, the temperature falls. As mass diffusion decreases, increasing the Schimdt number lowers the fluid's concentration. The relationship between velocity and Hartmann number is inverse. Suma *et al.* [12] studied the rate of heat transfer when using a rectangular lid-driven enclosure with a circular hollow cylinder for a nanofluid flow. As the Richardson number rises, so does the rate of heat transmission. A higher magnetic field improves fluid flow. Temperature increases with non-dimensional time. Irfan *et al*. [13] studied the effect of radiation in a bioconvective mode in fluid flow "Numerical study of nonlinear thermal radiation and Joule heating on MHD bioconvection Carreau nanofluid with gyrotactic microorganisms." Increasing Brownian diffusion raises the temperature. Hiking the Prandtl and Lewis numbers is given more attention. The biconvection Lewis number increases motile microorganisms. Suma *et al*. [14] studied "Optimization and sensitivity analysis of unsteady MHD mixed convective heat transfer in a lid-driven cavity containing a double-pipe circular cylinder using nanofluids." Heat transfer and non-dimensional time are related. When compared to heater length, fluid flow and Nusselt number are exactly related to the solid volume %. As the rate of application of the magnetic field increases, the Lorentz force reduces fluid flow. P. Deepalakshmi *et al.* [15] taking the couple stress into consideration made a detailed study on the fluid flow in a porous medium. Radiation and the slip parameter raise temperature, but the Prandtl number has the opposite effect. Heat diffusion has no effect on concentration. Heat source/sink and transfer rate are related, however radiation causes the reverse effect. Pressure decline is accelerated by the Hartmann number. Habiba *et al.* [16] used n-decane nanofluid for their study in a convective mode focusing on magnetic and radiation parameter. Fluid flow is analogous to Hartmann number. Nusselt number and vortex energy are enhanced by Richardson number. Radiation causes an increase in heat transfer. Many researchers [17-21] have contributed in this area of research.

Free convection is a process of heat transfer which happens naturally without any external force generally due to temperature gradient when the density differs. It has its application in the field of building designs, nuclear reactors etc., Hameed *et al.* [22] used Casson based Copper hydroxide nanofluid in a semi- parabolic surface. Rayleigh number increases heat and velocity transfer. The boundary layer thickens and the Nusselt number is increased by the corrugation number. The temperature drops by 8% because of the angle of inclination. Zeb *et al.* [23] used Prandtl fluid for their investigation. Pressure gradient is the opposite of velocity, which is exactly proportional to Prandtl numbers. The magnetic field reduces velocity. The application of radiation accelerates the rate of heat exchange. The concentration of the nanofluid rises as a result of a chemical reaction. Afifi *et al.* [24] used a hexagonal cavity with circular obstacles to study the rate of heat transfer in nanofluid. Hartmann number increasing in a range from 0 to 20, depletes the fluid flow as the maximum flow is obtained when it is at zero. Heat transferred by having a greater number of obstacles on Nusselt number. Maximum oscillation will lead to hike in velocity. When the obstacles are removed the stream function is at maximum. Saghafian *et al.* [25] applying heat flux constantly on vertical plate the rate of heat transfer was examined. Nusselt number is in corelation with maximum wall temperature. Mass flow increases with time but decreases with magnetic field and Hartmann number. Nciri *et al.* [26] investigated "Numerical Simulation of Natural Convection in a Chamfered Square Cavity with Fe3O4-Water Nanofluid and Magnetic Excitation." Temperature and velocity deaccelerate with Hartmann number.

Thermal radiation in nanofluid is rate of heat transfer through electromagnetic waves. It enhances heat transfer and also plays a vital role in the case of heat transfer where no contact is required. It has application in nuclear reactors, electronic cooling systems, etc. Ali *et al.* [27] used Casson fluid for their investigation to find out the effect of thermal radiations. Unsteady parameter, nanoparticle concentration, Casson fluid, Grashof number, Darcy number helps to increase velocity whereas magnetic field depletes it. Khan *et al*. [28] investigated "Impact of multiple slips and thermal radiation on heat and mass transfer in MHD Maxwell hybrid nanofluid flow over porous stretching sheet." Eckert number, thermal relaxation, velocity slip and Grashof number stimulates skin friction. Hybrid nanofluid possess more skin friction as compared to mono nanofluid. Deborah number, magnetic field, radiation and concentration slip parameters, all are responsible for the decline in Nusselt number. Grasshof number and radiation are inversely proportional to Sherwood number. Manjunatha *et al.* [29] made an investigation on the rate of heat transfer applying magnetic field and radiation. Solid volume fraction increased velocity. Temperature of clear fluid is more than nanofluid. Boundary layer thickness of

$Cu - water$ is more than that of clear fluid. When magnetic field is applied, rotation, heat source and skin friction increase. Alsemiry *et al.* [30] studied the Thermodiffusion Effects investigated on ANN-Based Prediction and RSM Optimization and applying couple stress. Dufour number accelerate temperature and rate of heat transfer. Velocity is enhanced by mixed convection and slip parameter. Khan *et al*. [31] studied the effect of thermal stratification on an inclined surface. Temperature increases for Deborah number but decreases for Prandtl number. Velocity depletes for Deborah number. Radiation and thermal stratification, boost temperature. Concentration of Fe_3O_4 in the fluid enhances temperature while it reduces velocity.

The stretching sheet in nanofluid flow refers to as the flat surface which keeps moving in a particular direction which generates boundary flow. It has its application in textile industry, thin film coating, biomedical engineering, etc. Li *et al.* [32] used ternary hybrid nanofluid in a Cattaneo-Christov heat flux model. Magnetic field when applied to the fluid, deaccelerated the velocity but increased the temperature and the boundary layer thickened. Biot number and Prandtl number increased the temperature while thermal relaxation brought down the temperature. Skin friction augmented by magnetic field. Mishra *et al.* [33] made an investigation in a spinning disk the effect of radiation. Due to magnetic field and porous matrix, the concentration of nanoparticles increases and hence oppose the fluid velocity and flow. There is great absorption of thermal radiation in the presence of silver nanoparticles leading to increase in temperature. Nusselt number is enhanced by radiation. Sait *et al.* [34] using electroosmotic effects with boundary slip studied the effect of the heat flow. Hartmann number increased the viscosity in the fluid leading to rise in pressure and shear stress while the temperature dropped. Velocity declined due to Prandtl numbers. Slip parameter and magnetic parameter have opposite actions on pressure gradient. Ouyang *et al.* [35] used ternary nanofluid for their study. Presence of nanoparticle increases the thermal conductivity in the fluid leading to rise in heat absorption. Suction/injection parameter has opposite effects on Nusselt number and temperature. Skin friction is enhanced by suction/injection factor.

Based on the reviewed literature, the authors are inspired to explore the boundary layer MHD stagnation point natural convection flow of a viscous, incompressible, electrically conducting, and heat radiating nanofluid past a stretchy surface with velocity slip and Newtonian heating in the presence of a transverse magnetic field. The primary objective of this study is to investigate the boundary layer MHD stagnation point natural convection flow and heat transfer characteristics of a viscous, incompressible, and electrically conducting nanofluid with thermal radiation effects. The analysis focuses on the influence of a transverse magnetic field, velocity slip, and Newtonian heating over a stretching surface, aiming to understand the combined impact of these parameters on the fluid flow and thermal behavior.

MATHEMATICAL MODEL

Consider the boundary layer, Magnetohydrodynamic (MHD), stagnation-point, natural convection flow of a viscous, incompressible, electrically conducting, and heat-radiating nanofluid past a stretching surface, in the presence of a uniform transverse magnetic field B_0. The x-axis is aligned along the horizontal direction of the stretching sheet, while the y-axis is perpendicular to it. Two equal and opposite forces act on the sheet, stretching it along its length with a velocity $U_w(x)$, keeping the origin fixed. The free-stream velocity of the nanofluid is taken as $U_\infty(x)$. The surface of the sheet is subject to convective heating from a hot fluid at temperature T_f, with a heat transfer coefficient h_f. The significant temperature difference between the ambient fluid temperature T_∞ and the boundary layer temperature T_w is assumed to generate substantial thermal radiation effects within the flow field. Partial velocity slip at the fluid–solid interface is considered, meaning the fluid velocity at the surface does not necessarily match the surface velocity due to slip effects. The magnetic Reynolds number of the nanofluid is assumed to be sufficiently small, allowing the neglect of any induced magnetic fields relative to the imposed magnetic field. The nanoparticle volume fraction at the sheet's surface and far from the boundary layer are denoted by C_w and C_∞ , respectively.

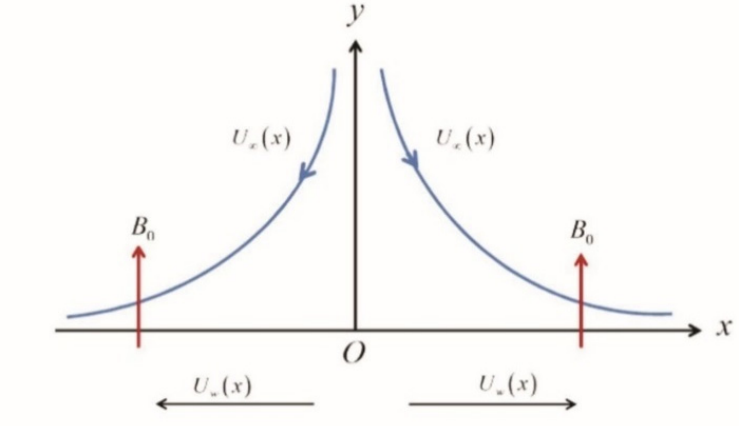

Figure 1. Schematic diagram of the physical configuration

Based on the assumptions aforementioned, equations governing to the present problem, using Rosseland's approximation, are given by:

$$\frac{\partial u}{\partial x}+\frac{\partial v}{\partial y}=0 \tag{1}$$

$$u\frac{\partial u}{\partial x}+v\frac{\partial u}{\partial y}=\upsilon\frac{\partial^2 u}{\partial y^2}+U_\infty\frac{\partial U_\infty}{\partial x}+\frac{\sigma B_0^2}{\rho_f}(U_\infty-u)+\frac{1}{\rho_f}\left[(1-C_\infty)\rho_{f\infty}\beta g(T-T_\infty)-(\rho_p-\rho_{f\infty})g(C-C_\infty)\right] \tag{2}$$

$$u\frac{\partial T}{\partial x}+v\frac{\partial T}{\partial y}=\alpha_m\frac{\partial^2 T}{\partial y^2}+\tau\left\{D_B\frac{\partial C}{\partial y}\frac{\partial T}{\partial y}+\frac{D_T}{T_\infty}\left(\frac{\partial T}{\partial y}\right)^2\right\}+\frac{\partial}{\partial y}\left(\frac{16\sigma^* T^3}{3\alpha^*}\frac{\partial T}{\partial y}\right) \tag{3}$$

$$u\frac{\partial C}{\partial x}+v\frac{\partial C}{\partial y}=D_B\frac{\partial^2 C}{\partial y^2}+\frac{D_T}{T_\infty}\frac{\partial^2 T}{\partial y^2} \tag{4}$$

where u and v are the velocity components along the x and y axes, respectively, $\alpha_m=\dfrac{k}{(\rho c)_f}$ is the thermal diffusivity of the fluid, υ is the kinematic viscosity, D_B is the Brownian diffusion coefficient, D_T is the thermophoretic diffusion coefficient and $\tau=\dfrac{(\rho c)_p}{(\rho c)_f}$ is the ratio between the effective heat capacity of the nanoparticle material and heat capacity of the fluid with ρ being the density, c is the specific heat at constant pressure, ρ_p is the density of the particles, $\sigma*$ is the Stefan-Boltzmann constant, $\alpha*$ is the Rosseland mean absorption coefficient.

The current situation is governed by the following boundary conditions:

$$\left.\begin{aligned} &u=U_w+L\frac{\partial u}{\partial y}=cx+L\frac{\partial u}{\partial y},\ v=0,\ -k\frac{\partial T}{\partial y}=h(T_f-T),\ C=C_w \quad \text{at} \quad y=0\\ &u\to U_\infty=ax,\ v=0,\ T\to T_\infty,\ C\to C_\infty \quad \text{at} \quad y\to\infty \end{aligned}\right\} \tag{5}$$

where $U_w=c\,x\ (c>0)$, L, k, and $U_\infty=ax\ (a>0)$ are, respectively, the velocity of the stretching sheet, slip length, thermal conductivity of the nanofluid, and free stream velocity of the nanofluid.

The dimensionless and similarity variables are listed below:

$$\eta=y\sqrt{\frac{a}{\upsilon}},\quad \psi=\sqrt{a\upsilon}\,x\,f(\eta),\qquad \theta(\eta)=\frac{T-T_\infty}{T_f-T_\infty},\quad \phi(\eta)=\frac{C-C_\infty}{C_w-C_\infty} \tag{6}$$

Equation (1) is satisfied in the same way that equation (6) is applied. The following are the types of equations (2), (3), and (4), as well as the boundary conditions (5):

$$f'''+ff''-f'^2+1+M\left(1-f'\right)+Gr\,\theta-Nr\,\phi=0 \tag{7}$$

$$\left[1+\frac{4}{3N_R}\left\{1+(\theta_w-1)\theta\right\}^3\right]\theta''+\Pr f\theta'+\Pr Nb\phi'\theta'+\left[\Pr Nt+\frac{4}{N_R}(\theta_w-1)\left\{1+(\theta_w-1)\theta\right\}^2\right]\theta'^2=0 \tag{8}$$

$$\phi''+Le\Pr f\phi'+\frac{Nt}{Nb}\theta''=0 \tag{9}$$

Boundary conditions are used in non-dimensional formats as

$$\left.\begin{aligned} &f(\eta)=0,\ f'(\eta)=\alpha+Af''(\eta),\ \ \theta'(\eta)=-Bi[1-\theta(\eta)],\ \ \phi(\eta)=1,\ \text{at}\ \eta=0\\ &f'(\eta)\to 1,\ \ \theta(\eta)\to 0,\ \ \phi(\eta)\to 0\ \ \text{at}\ \eta\to\infty. \end{aligned}\right\} \tag{10}$$

The non-dimensional governing parameters in this case are defined as follows:

$$\left.\begin{aligned} &M=\frac{\sigma B_o^2}{\rho_f a},\ Le=\frac{\alpha}{D_B},\ \Pr=\frac{\upsilon}{\alpha},\ \alpha=\frac{c}{a},\ A=L\sqrt{\frac{a}{\upsilon}},\ \ Nb=\frac{(\rho c)_p D_B(C_w-C_\infty)}{(\rho c)_f\upsilon},\ \ Nt=\frac{(\rho c)_p D_T(T_m-T_\infty)}{(\rho c)_f\upsilon T_\infty},\\ &Gr=\frac{(1-C_\infty)\beta\rho_{f\infty}\,g(T_m-T_\infty)}{\rho_f U_\infty a},\ Nr=\frac{(\rho_p-\rho_{f\infty})g(C_w-C_\infty)}{\rho_f U_\infty a},\ N_R=\frac{k\alpha^*}{4\sigma* T_\infty^{\,3}},\ \theta_w=\frac{T_w}{T_\infty},\ Bi=\frac{h}{k}\sqrt{\frac{\upsilon}{\alpha}}. \end{aligned}\right\} \tag{11}$$

where M, Le, Pr, α, A, Nb, Nt, Gr, Nr, N_R, θ_w, Bi are, respectively, the magnetic parameter, Lewis number, Prandtl number, ratio of rates of stretching velocity and free stream velocity, velocity slip parameter, Brownian motion parameter, thermophoresis parameter, thermal Grashof number, solutal Grashof number, radiation parameter, temperature ratio parameter, and Biot number.

On the basis of above quantities, the coefficient of skin friction C_f, local Nusselt number Nu_x, and local Sherwood number Sh_x are defined as:

$$C_f = \frac{\tau_w}{\rho u_w^{\,2}},\ Nu_x = \frac{x q_w}{k\left(T_m - T_\infty\right)},\ Sh_x = \frac{x h_m}{D_B\left(C_w - C_\infty\right)} \tag{12}$$

where the wall shear stress τ_w, wall heat-flux q_w and wall mass-flux h_m are given by

$$\tau_w = \mu\left(\frac{\partial u}{\partial y}\right)_{y=0},\ q_w = -k\left(\frac{\partial T}{\partial y}\right)_{y=0},\ h_m = -D_B\left(\frac{\partial C}{\partial y}\right)_{y=0}. \tag{13}$$

We get the following results by using similar variables and the above equations.

$$C_f\sqrt{\mathrm{Re}_x} = f''(0),\ \frac{Nu_x}{\sqrt{\mathrm{Re}_x}} = -\theta'(0),\ \frac{Sh_x}{\sqrt{\mathrm{Re}_x}} = -\phi'(0) \tag{14}$$

where Re_x is the local Reynolds number.

NUMERICAL PROCEDURE

Non-linear ordinary differential equations are found from the controlling non-linear partial differential equations (1) - (5) with the help of suitable similarity transformation. These equations (7) - (9) together with boundary conditions (10) are solved, numerically, using MATLAB's bvp4c routine. To confirm robustness and accuracy of the result, the same scheme is applied to the present problem taking $Gr = Nr = 0$ and the numerical values of coefficient of skin-friction, Nusselt number and Sherwood number has been calculated and compared with the results obtained by Mahatha *et al*. [36], and they are found to be in good agreement.

Table 1. Computations showing comparison with Mahatha *et al*. [36] taking $Gr = Nr = 0$.

								Mahatha *et al*. [36]			**Present Finding**		
M	N_r	θ_w	Nb	Nt	α	A	Bi	$-C_f\sqrt{\mathrm{Re}_x}$	$\frac{Nu_x}{\sqrt{\mathrm{Re}_x}}$	$\frac{Sh_x}{\sqrt{\mathrm{Re}_x}}$	$-C_f\sqrt{\mathrm{Re}_x}$	$\frac{Nu_x}{\sqrt{\mathrm{Re}_x}}$	$\frac{Sh_x}{\sqrt{\mathrm{Re}_x}}$
2	5	2	0.1	0.1	2	0.5	0.5	1.0559954	0.56564827	1.9085476	1.0559954	0.56564827	1.9085476
6								1.19783053	0.56360081	1.85031759	1.19783053	0.56360081	1.85031759
10								1.28411476	0.56236343	1.81727632	1.28411476	0.56236343	1.81727632
	5							1.05599540	0.56564827	1.90854760	1.05599540	0.56564827	1.90854760
	10							1.05599540	0.47273451	1.89617746	1.05599540	0.47273451	1.89617746
	15							1.05599540	0.44257262	1.89169667	1.05599540	0.44257262	1.89169667
		2						1.05599540	0.56564827	1.90854760	1.05599540	0.56564827	1.90854760
		3						1.05599540	0.73300040	1.94109901	1.05599540	0.73300040	1.94109901
		4						1.05599540	1.09573572	1.98983165	1.05599540	1.09573572	1.98983165
			0.1					1.05599540	0.56564827	1.90854760	1.05599540	0.56564827	1.90854760
			0.2					1.05599540	0.54620893	2.00630565	1.05599540	0.54620893	2.00630565
			0.3					1.05599540	0.52186269	2.03933398	1.05599540	0.52186269	2.03933398
				0.1				1.05599540	0.56564827	1.90854760	1.05599540	0.56564827	1.90854760
				0.3				1.05599540	0.55916364	1.69574713	1.05599540	0.55916364	1.69574713
				0.5				1.05599540	0.55107685	1.57321616	1.05599540	0.55107685	1.57321616
					1.5			0.52197609	0.56129753	1.79227818	0.52197609	0.56129753	1.79227818
					2.0			1.05599540	0.56564827	1.90854760	1.05599540	0.56564827	1.90854760
					2.5			1.60080045	0.56927362	2.01863199	1.60080045	0.56927362	2.01863199
						0.1		1.87844309	0.57087930	2.07184081	1.87844309	0.57087930	2.07184081
						0.3		1.34862035	0.56768153	1.96865917	1.34862035	0.56768153	1.96865917
						0.5		1.05599540	0.56564827	1.90854760	1.05599540	0.56564827	1.90854760
							0.5	1.05599540	0.56564827	1.90854760	1.05599540	0.56564827	1.90854760
							1.0	1.05599540	0.99831813	1.86710996	1.05599540	0.99831813	1.86710996
							1.5	1.05599540	1.31203155	1.85838165	1.05599540	1.31203155	1.85838165

RESULTS AND DISCUSSION

To get insight into the flow pattern, the effects of various flow parameters on fluid velocity, temperature and concentration have been depicted in graphical form from Figures 2-37. It is evident from Fig. 2-13 that on increasing M, θ_w, A, N_r, there is a decrease in fluid velocity while on increasing Nb, Nt, α, Bi, Le, Gr, N_R and Pr, an increment on fluid velocity is seen. This implies that magnetic field, temperature ratio, velocity slip, solutal Grasshof number have the tendency to retard the fluid velocity while Brownian diffusion, thermophoretic diffusion, stretching ratio, convective heating, Lewis number, thermal Grasshof number, non-linear radiation and Prandtl number have the reverse

effect on it. The application of a transverse magnetic field induces a Lorentz force that opposes the motion of the electrically conducting fluid, acting as a resistive (drag) force and thereby reducing the fluid velocity. Though typically promoting flow due to solutal buoyancy, under certain conditions (e.g., adverse concentration gradients), it may counteract thermal buoyancy, thereby slowing the flow. Brownian diffusion enhances nanoparticle motion, which contributes to increased thermal conductivity and energy transport, indirectly supporting momentum transfer and increasing velocity. Thermophoretic diffusion drives nanoparticles away from heated regions, enhancing momentum in the fluid layers and increasing the overall velocity. Greater surface heating enhances buoyancy-driven flow, thus increasing velocity on increasing convective heating. Thermal Grashof number represents buoyancy effects due to temperature differences. Higher values increase upward motion and accelerate fluid flow. Radiative heat enhances thermal energy in the system, increasing buoyancy and promoting fluid acceleration.

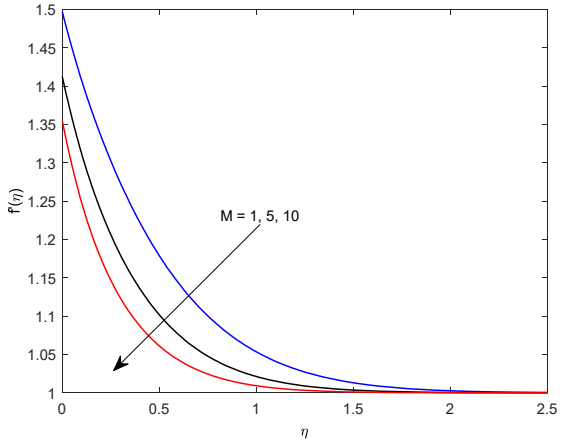

Figure 2. Velocity profile for M

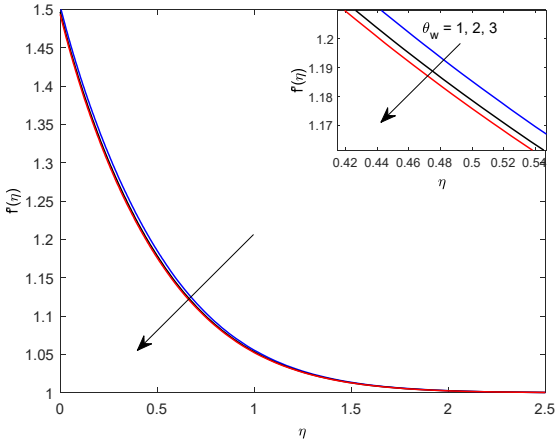

Figure 3. Velocity profile for θ_w

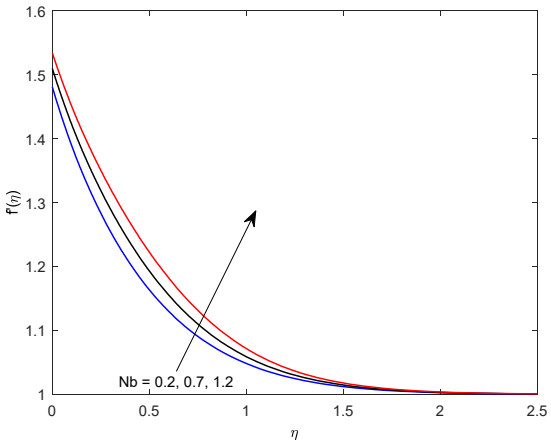

Figure 4. Velocity profile for Nb

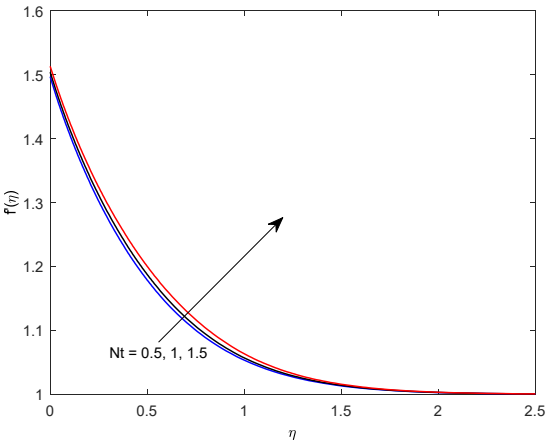

Figure 5. Velocity profile for Nt

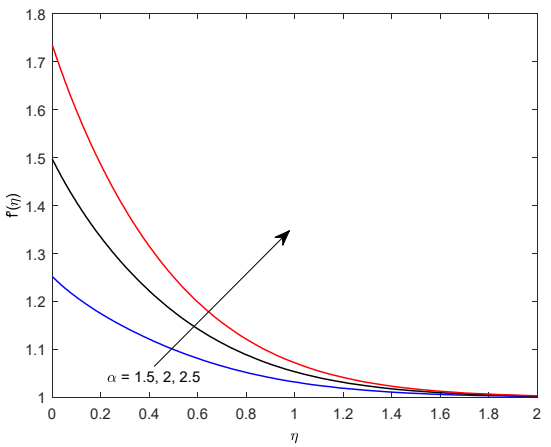

Figure 6. Velocity profile for α

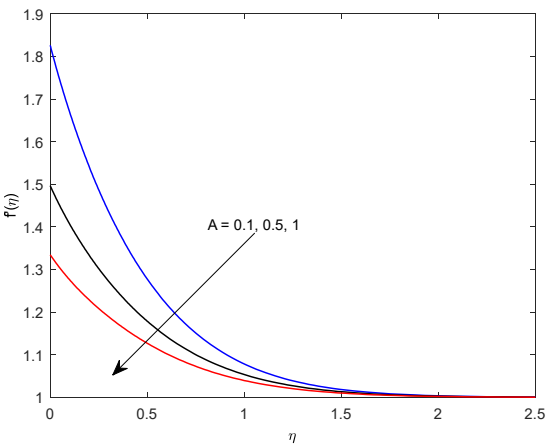

Figure 7. Velocity profile for A

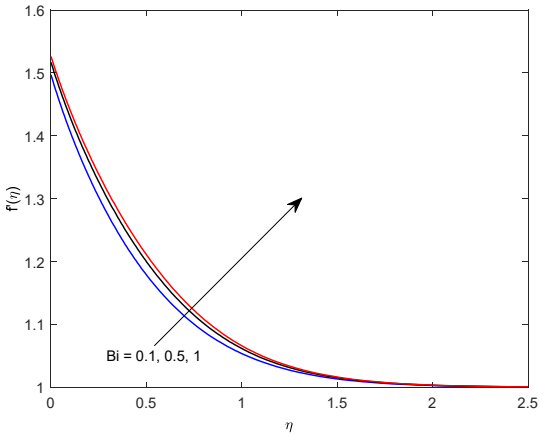

Figure 8. Velocity profile for Bi

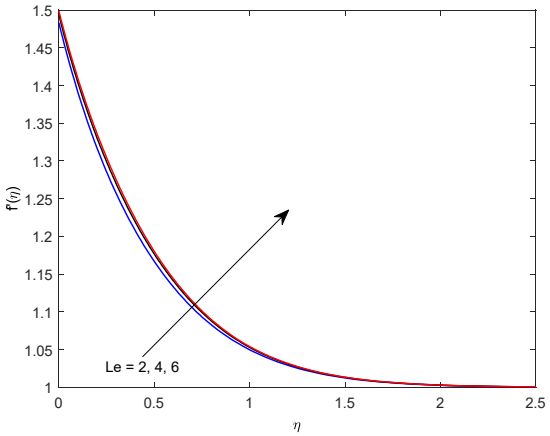

Figure 9. Velocity profile for Le

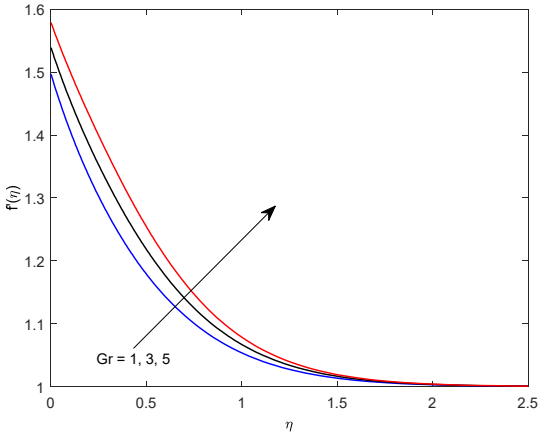

Figure 10. Velocity profile for Gr

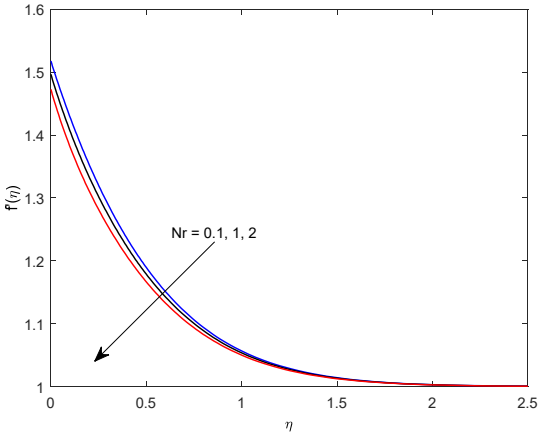

Figure 11. Velocity profile for Nr

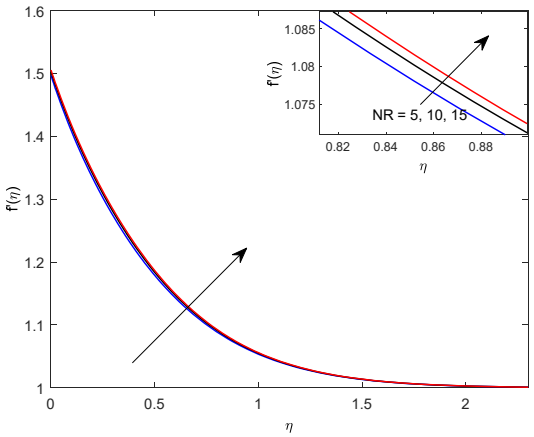

Figure 12. Velocity profile for N_R

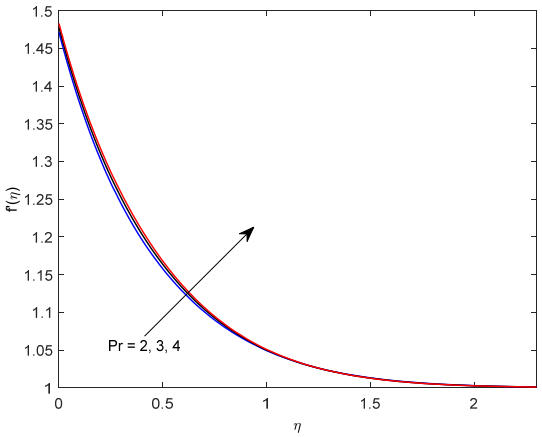

Figure 13. Velocity profile for Pr

Figs. 14-25 represents the effects of various flow parameters on fluid temperature. It is clearly seen from fig. 14-25 that on increasing M, Nb, Nt, A, Bi, Le, Nr, N_R and Pr, fluid temperature is getting increased while it is decreasing θ_w, α, Gr. This implies that the fluid temperature is getting enhanced by Brownian diffusion, thermophoretic diffusion, velocity slip, convective heating, Lewis number, non-linear thermal radiation and Prandtl number. While reverse trend is visible in temperature profiles for temperature ratio, stretching ratio and thermal Grasshof number. Brownian motion of nanoparticles enhances random thermal agitation within the fluid, promoting increased thermal conductivity and leading to a rise in fluid temperature. Thermophoresis causes particles to move from hot to cold regions, redistributing energy within the boundary layer. This enhances the thermal boundary layer thickness and increases the temperature. Stronger convective heating at the surface introduces more heat into the fluid, increasing its temperature near the wall and throughout the boundary layer. Thermal radiation provides an additional mode of energy transport. With nonlinear radiation, this effect becomes more pronounced at higher temperatures, leading to significant heat gain in the fluid. While

Gr promotes buoyancy-driven flow, a high *Gr* accelerating the fluid away from the heated surface, reducing residence time and resulting in lower temperatures within the thermal boundary layer.

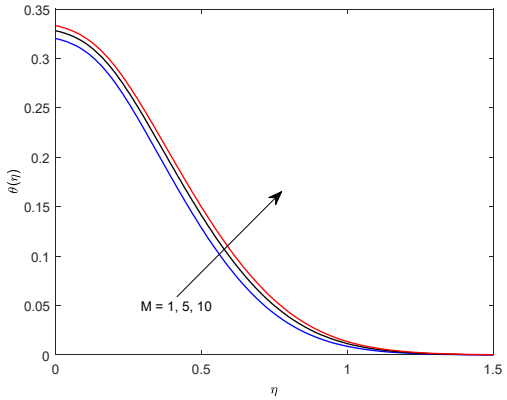

Figure 14. Temperature profile for M

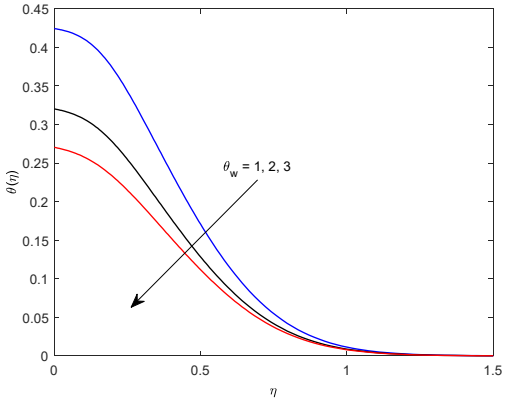

Figure 15. Temperature profile for θ_w

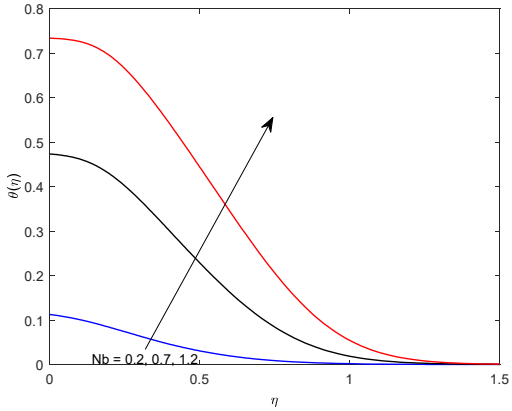

Figure 16. Temperature profile for Nb

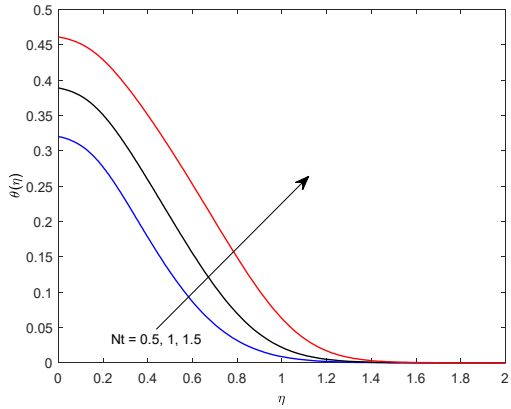

Figure 17. Temperature profile for Nt

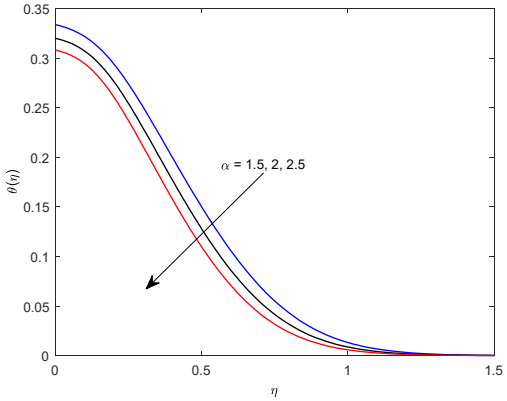

Figure 18. Temperature profile for α

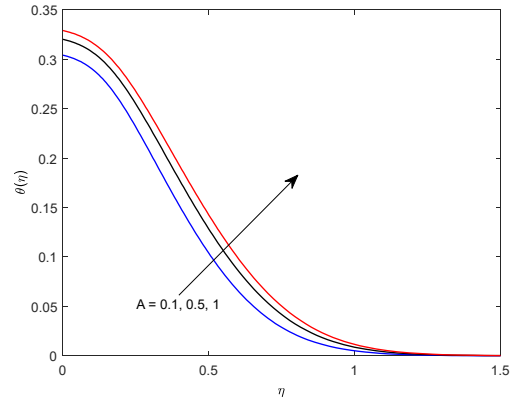

Figure 19. Temperature profile for A

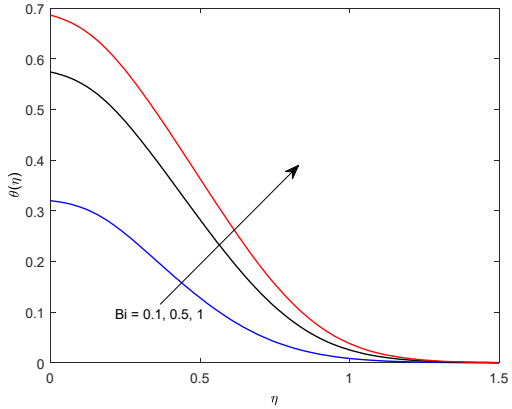

Figure 20. Temperature profile for *Bi*

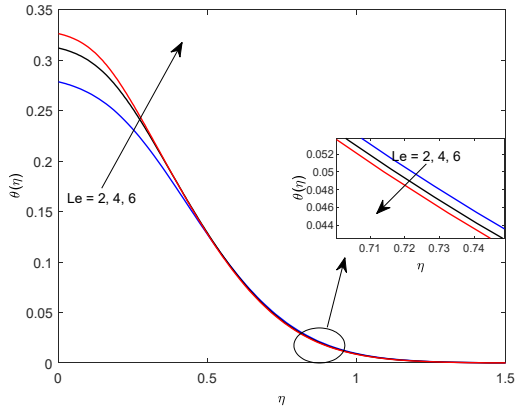

Figure 21. Temperature profile for Le

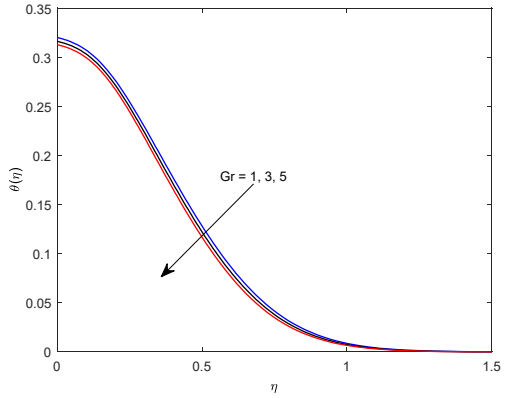

Figure 22. Temperature profile for Gr

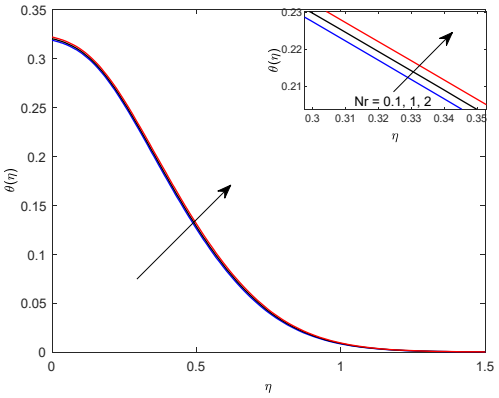

Figure 23. Temperature profile for Nr

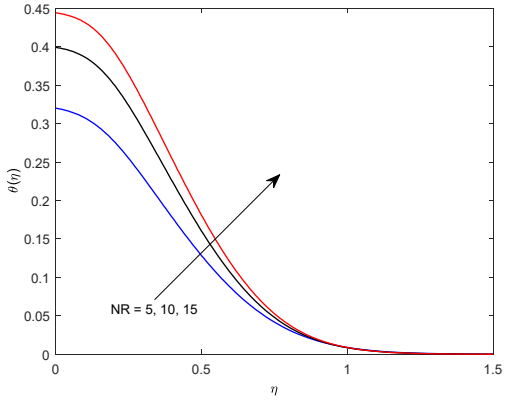

Figure 24. Temperature profile for N_R

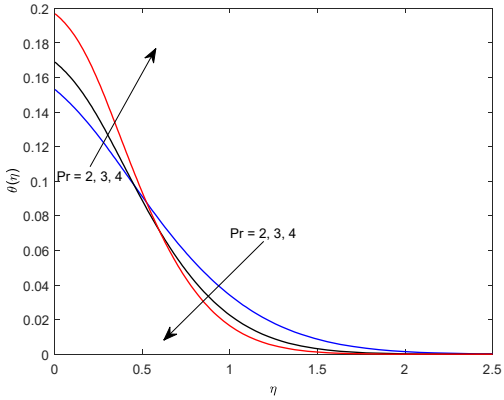

Figure 25. Temperature profile for Pr

It is visible from Fig. 26-37 that with the increase in M, θ_w, A, Nr, there is an increment in the concentration profiles while there is a decrement on increasing Nb, Nt, α, Bi, Le, Gr, N_R and Pr in the boundary layer region.

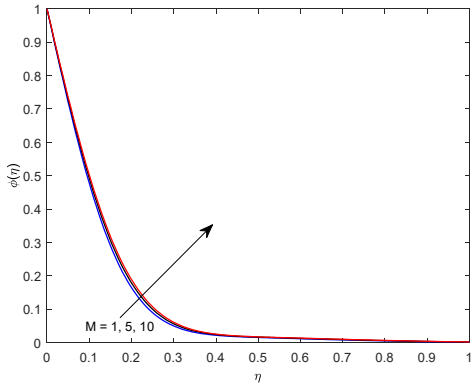

Figure 26. Concentration profile for M

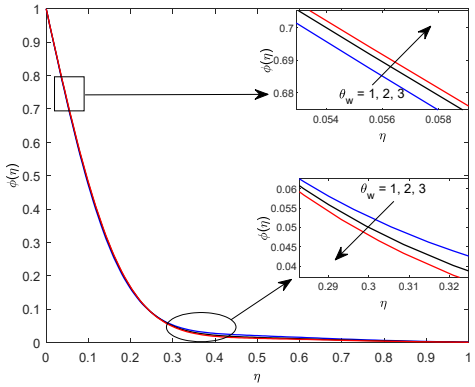

Figure 27. Concentration profile for θ_w

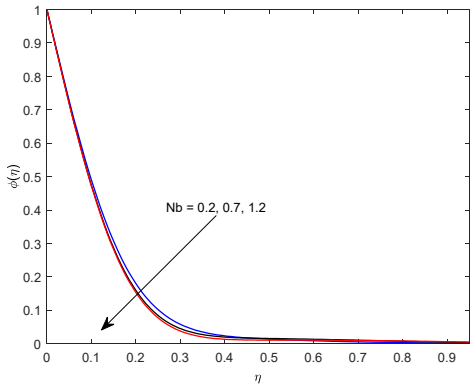

Figure 28. Concentration profile for Nb

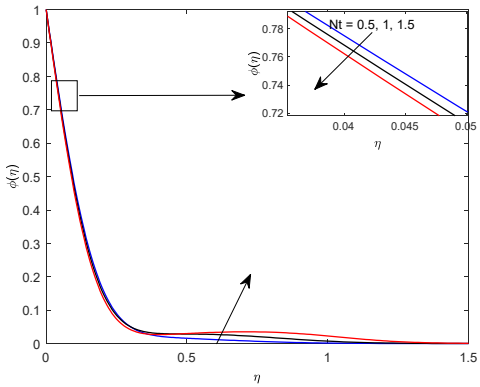

Figure 29. Concentration profile for Nt

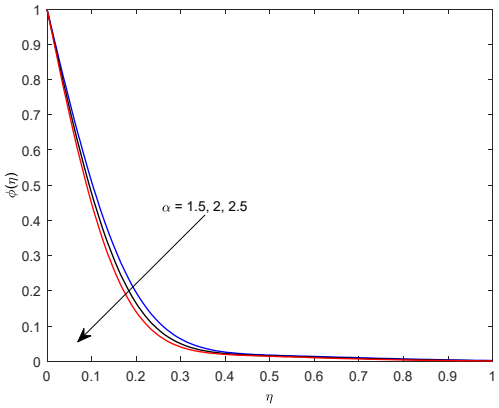

Figure 30. Concentration profile for α

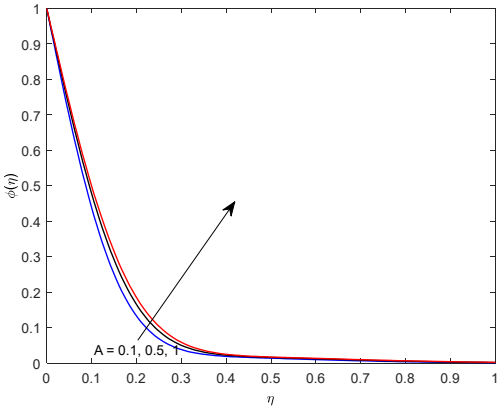

Figure 31. Concentration profile for A

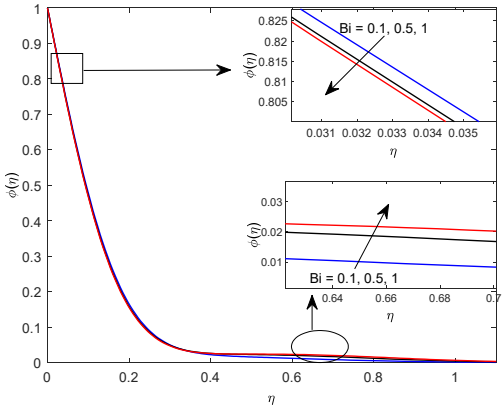

Figure 32. Concentration profile for Bi

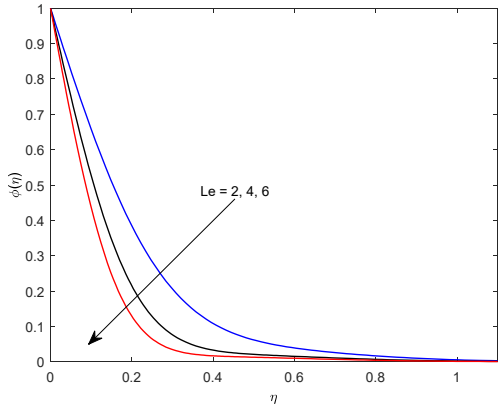

Figure 33. Concentration profile for Le

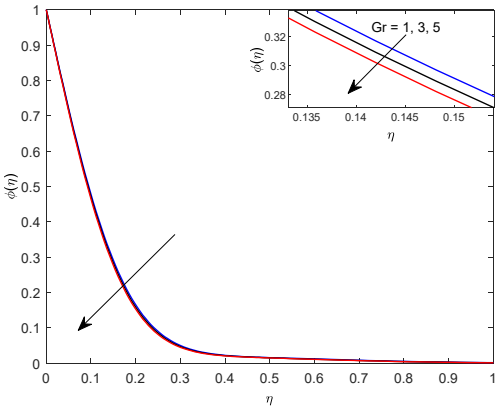

Figure 34. Concentration profile for Gr

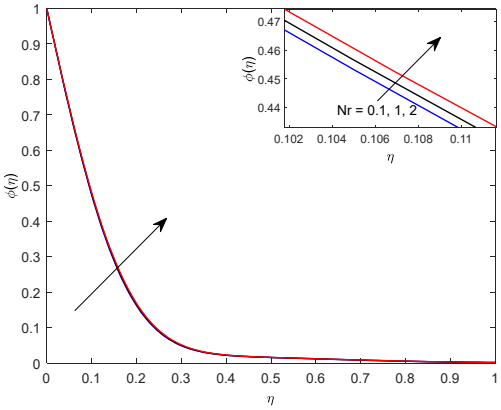

Figure 35. Concentration profile for Nr

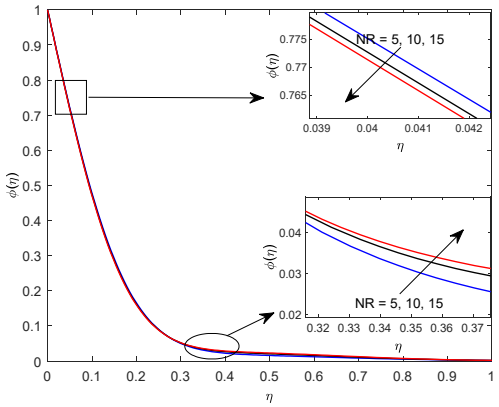

Figure 36. Concentration profile for N_R

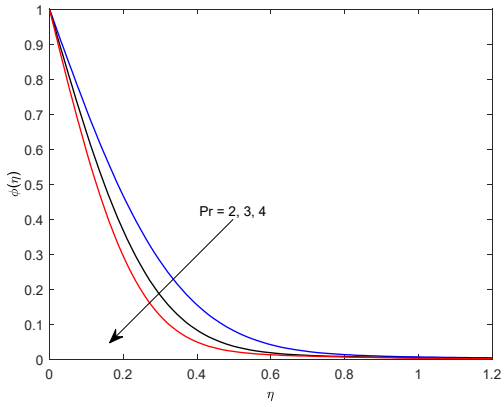

Figure 37. Concentration profile for Pr

This shows that the magnetic field, temperature ratio, velocity slip and solutal Grasshof number are the cause for the rise in concentration of fluid. On the other hand, Brownian motion, thermophoretic diffusion, stretching parameter,

Newtonian heating, Lewis number, Grasshof number, Prandtl number and non-linear radiation. These are the cause in concentration profile. The application of a magnetic field generates a Lorentz force that opposes fluid motion. This suppresses convective transport and slows the fluid, allowing more time for mass to accumulate near the surface, thereby increasing concentration. As solutal Grashof number measures buoyancy effects due to concentration differences. A higher value promotes solutal buoyancy-driven flow, which enhance concentration near the surface due to a stronger diffusion gradient. Brownian diffusion promotes random motion of nanoparticles, which tends to spread out concentration gradients and leads to a decrease in the local concentration near the surface. Thermophoresis drives particles from hot to cold regions, often away from the surface, thereby reducing the concentration in the boundary layer. Strong surface heating increases thermal energy, which activate both thermophoretic and Brownian effects, enhancing mass diffusion and reducing concentration near the wall. Enhanced buoyancy due to temperature differences promotes faster upward fluid motion, which dilutes concentration near the surface by enhancing convective mass transport. A high Prandtl number implies slower thermal diffusion, which may indirectly increase convective effects and enhance species dispersion, thus lowering concentration. Increased radiative heat flux intensifies temperature gradients, which promote stronger thermophoretic effects, pushing nanoparticles away from the wall and decreasing concentration in the near-wall region.

To get more physical insight, the effects of various physical entities on skin friction, rate of heat transfer and rate of mass transfer have been calculated and listed in Table 2.

Table 2. Numerical values of the coefficient of skin friction, Nusselt number and Sherwood number against different values of flow parameters

M	N_R	θ_w	Pr	Nb	Nt	α	A	Bi	Le	Gr	Nr	$C_f\sqrt{\mathrm{Re}_x}$	$\mathrm{Re}_x^{-1/2}Nu_x$	$\mathrm{Re}_x^{-1/2}Sh_x$
1	5	2	6.785	0.5	0.5	2	0.5	0.1	5	1	1	1.00647243	0.10969678	5.71847394
5												1.17545046	0.10916806	5.52978961
10												1.29087133	0.10881602	5.40032863
	5											1.00647243	0.10969678	5.71847394
	10											0.99539217	0.08202349	5.78274036
	15											0.98883774	0.0704694	5.81704256
		1										0.99178448	0.07291539	5.80510782
		2										1.00647243	0.10969678	5.71847394
		3										1.01305281	0.14412317	5.67286711
			2									1.05697201	0.11931776	2.94310389
			3									1.04442418	0.11850775	3.66004079
			4									1.03394039	0.1170332	4.27679022
				0.2								1.03810586	0.12133854	5.59760324
				0.7								0.98054756	0.09757684	5.74929635
				1.2								0.93176267	0.06360343	5.76595794
					0.5							1.00647243	0.10969678	5.71847394
					1							0.9919851	0.10477874	5.90396126
					1.5							0.9735596	0.09873209	6.06812004
						1.5						0.49631091	0.10877109	5.28764785
						2						1.00647243	0.10969678	5.71847394
						2.5						1.53026552	0.11047703	6.11135321
							0.1					1.73817223	0.11074986	6.2560944
							0.5					1.00647243	0.10969678	5.71847394
							1					0.66538584	0.10909963	5.43657748
								0.1				1.00647243	0.10969678	5.71847394
								0.3				0.96674662	0.26068122	5.83954402
								0.5				0.94784719	0.35745004	5.88242681
									2			1.03339216	0.11235762	3.57004164
									4			1.01203843	0.11024239	5.10455488
									6			1.002337	0.1092959	6.27206578
										1		1.00647243	0.10969678	5.71847394
										3		0.92209211	0.10994859	5.81105052
										5		0.84229688	0.11017426	5.89685957
											0.1	0.9640686	0.10979618	5.76159899
											1	1.00647243	0.10969678	5.71847394
											2	1.05443945	0.10958192	5.66923073

It is evident from Table 2 that the skin friction is getting hiked by magnetic field, temperature ratio, stretching ratio and linear non-thermal radiation whereas it experiences reverse effect by solutal Grasshof number, Prandtl number, Brownian motion, thermophoretic diffusion, velocity slip, convective heating, Lewis number and thermal Grasshof number. The Lorentz force acts against the flow, increasing resistance and thereby enhancing wall shear stress, which

leads to higher skin friction Increased stretching of the surface amplifies tangential stress and fluid acceleration near the wall, raising skin friction. Radiation alters energy distribution in the flow, potentially increasing momentum transfer near the surface, which raises wall shear stress. Enhanced solutal buoyancy may weaken the surface shear due to rising flow, leading to a drop in friction at the wall. Higher Pr reduces thermal diffusivity, thinning the velocity boundary layer and thereby reducing friction drag. Brownian motion and thermophoretic diffusion disrupt the uniformity of momentum transport, reducing shear at the wall. Slip condition reduces direct contact between the fluid and surface, decreasing the frictional force. Convective heating increases thermal energy and buoyancy, which may redistribute momentum and reduce skin friction. Strong thermal buoyancy lifts fluid away from the wall, reducing wall shear stress.

Temperature ratio, stretching ratio, convecting heating and thermal Grasshof number have the tendency to enhance the rate of heat transfer at the surface while magnetic field, solutal Grasshof number, Prandtl number, Brownian motion, thermophoretic diffusion, velocity slip, Lewis number and thermal radiation have a reverse effect on heat transfer. A higher wall temperature promotes a stronger thermal gradient, enhancing heat transfer. Stretching increases convective effects, improving surface heat transfer. Convective heating directly enhances surface heat input, increasing the temperature gradient and rate of heat transfer. Thermal Grashof number boosts thermal buoyancy-driven convection, enhancing heat transfer from the surface. The resistive Lorentz force suppresses fluid motion, weakening convection and reducing heat transfer. Solutal Grashof Number may oppose thermal buoyancy in some regimes, reducing heat transfer effectiveness. Higher Pr means lower thermal diffusivity, resulting in thinner thermal boundary layers, which can reduce heat transfer if the flow is not accelerated proportionally. Brownian motion and thermophoretic diffusion increase thermal boundary layer thickness due to nanoparticle interactions, reducing the surface heat gradient. Velocity Slip decreases the transfer of thermal energy from the wall to fluid. Nonlinear thermal radiation reduces the effective thermal gradient at the wall by redistributing heat into the fluid bulk, lowering surface heat flux. Solutal Grasshof number, Prandtl number, Brownian diffusion, thermophoretic diffusion, stretching ratio, Newtonian heating, Lewis number and thermal Grasshof number accelerate the rate of mass transfer whereas magnetic field, temperature ratio, velocity slip and thermal radiation deaccelerate the rate of mass transfer. Solutal Grashof number enhances concentration-driven buoyancy, promoting species transport and increasing mass transfer rate. Brownian motion and thermophoretic diffusion intensify particle diffusion and migration, thus enhancing mass transfer at the wall. Newtonian heating promotes both thermal and concentration gradients, especially when mass transfer is coupled with temperature effects. Thermal Grashof number boosts upward convection, carrying species away from the surface and enhancing mass transfer. Magnetic field slows fluid motion due to Lorentz force, reducing convective mass transport. Temperature ratio may alter thermal stratification, diminishing thermophoretic effects and lowering mass transfer. Velocity slip reduces surface interaction, limiting mass exchange between the surface and fluid. Thermal radiation alters temperature distribution, which affects species migration driven by thermal gradients, potentially weakening mass transfer.

CONCLUSIONS

The present study comprehensively investigates the influence of various flow parameters on the velocity, temperature, and concentration fields, as well as on the skin friction coefficient, rate of heat transfer, and rate of mass transfer in a boundary layer MHD stagnation-point flow of a nanofluid over a stretching surface, incorporating velocity slip, Newtonian heating, and thermal radiation effects. The key conclusions drawn from the study are summarized below:

- “Due to enhanced resistive or damping forces, magnetic field, temperature ratio, velocity slip, and solutal Grashof number reduces the nanofluid velocity. On the other hand, convective heating, thermal Grashof number, nonlinear radiation, and Prandtl number induces the nanofluid velocity, owing to strengthened convective or thermal driving mechanisms”.
- “Fluid temperature is increased by Brownian motion, thermophoretic diffusion, velocity slip, convective heating, nonlinear thermal radiation, and Prandtl number, as these enhance thermal energy accumulation or diffusion whereas it is decreased with increasing temperature ratio, and thermal Grashof number due to the thinning of the thermal boundary layer or enhanced convective cooling”.
- “An increase in nanofluid concentration profiles on increasing magnetic field, temperature ratio, velocity slip, and solutal Grashof number, indicating suppressed mass diffusion or accumulation near the wall. On the other hand, decreased concentration is observed with increasing Newtonian heating, thermal Grashof number, Prandtl number, and nonlinear radiation due to enhanced mass diffusion or particle migration away from the surface”.
- “Due to enhanced resistive or surface-driven momentum input, magnetic field, temperature ratio, and linear non-thermal radiation enhances the skin friction while a reduction due to solutal Grashof number, Prandtl number, Brownian motion, thermophoretic diffusion, velocity slip, convective heating, Lewis number, and thermal Grashof number, indicates momentum thinning or reduced wall interaction”.
- “Rate of heat transfer is getting enhanced by temperature ratio, convective heating, and thermal Grashof number due to increased thermal gradients and buoyancy-driven heat transport whereas it is reduced by magnetic field, solutal Grashof number, Prandtl number, Brownian motion, thermophoretic diffusion, velocity slip, and thermal radiation, owing to boundary layer thickening or damping effects”.
- “Mass transfer increases with solutal Grashof number, Prandtl number, Brownian motion, thermophoretic diffusion, Newtonian heating, and thermal Grashof number due to intensified concentration gradients and diffusive transport.

It decreases with magnetic field, temperature ratio, velocity slip, and thermal radiation, reflecting inhibited mass transport and particle dispersion".

ORCID

G.K. Mahato, https://orcid.org/0000-0003-4549-0042

REFERENCES

[1] M. Nandini, B.N. Hanumagowda, G. Saini, S.V.K. Varma, J.V. Tawade, N.V. Satpute, R. Ghodhbani, *et al*., "Non-linear thermal radiation impacts on MHD nanofluid flow in a rotating channel with Darcy-forccheimer model:An entropy analysis," J. Rad. Res. Appl. Sci. **18**(1), 101228 (2025). (2024). https://doi.org/10.1016/j.jrras.2024.101228

[2] Y. Ouyanga, Md. Faisal, Md. Basir, K. Naganthran, and I. Pop, "Numerical analysis of MHD ternary nanofluid flow past a permeable stretching/shrinking sheet with velocity slip," Alexandria Engineering Journal, **116**, 427-438 (2025). https://doi.org/10.1016/j.aej.2024.12.089

[3] Md.M. Hasan, M.J. Uddin, and S.A. Faroughi, "Magnetohydrodynamic nanofluids flow and heat transfer with radiative heat flux and exothermic chemical reactions," International Journal of Thermofluids, **26**, 101114 (2025). https://doi.org/10.1016/j.ijft.2025.101114

[4] Shilpa, R. Mehta, and K. Senthilvadivu, "Artificial neural network analysis on heat and mass transfer in MHD Carreau ternary hybrid nanofluid flow across a vertical cylinder: A numerical computation," International Journal of Thermofluids, **27**, 101171 (2025). https://doi.org/10.1016/j.ijft.2025.101171

[5] Z.H. Khan, O.D. Makinde, M. Usman, A. Rashid, and W.A. Khan, Fractional order analysis of radiating couple stress MHD nanofluid flow in a permeable wall channel. Journal of Taibah University for Science, **19**(1), 2485396 (2025). https://doi.org/10.1080/16583655.2025.2485396

[6] H. Vaidya, M. Bakouri, D. Tripathi, I. Khan, A.M. Alqahtani, K.V. Prasad, and R. Choudhari, "Significance of thermal radiation on peristaltic flow of Phan-Thien-Tanner MHD nanofluid containing gold nanoparticles with applications in cancer medications," Journal of Radiation Research and Applied Sciences, **18**(1), 101212 (2024). https://doi.org/10.1016/j.jrras.2024.101212

[7] E.O. Fatunmbi, A.M. Obalalu, S.O. Salawu, U. Khand, N. Abdullah, S, Elattar, and R. Ghodhbani, Refka, "Aspects of heat transfer hybridized micropolar water-based iron oxide and silver nanoparticles across a stretching bidirectional sheet with thermal radiation," Journal of Radiation Research and Applied Sciences, **18**, 101220 (2024). https://doi.org/10.1016/j.jrras.2024.101220

[8] S. Saranya, P. Ragupathi, and Q.M. Al-Mdallal, "Impact of micropolar effects on nanofluid flow between two disks," International Journal of Thermo-fluids, **26**, 101050 (2025). https://doi.org/10.1016/j.ijft.2024.101050

[9] M.A. Iqbal, N. Khan, A.H. Alzahrani, and Y. Khan, "Thermophoretic particle deposition in bioconvection flow of nanofluid with microorganisms and heat source: Applications of nanoparticle and thermal radiation," Journal of Radiation Research and Applied Sciences, **18**, 101305 (2025). https://doi.org/10.1016/j.jrras.2025.101305

[10] M.S. Alqurashi, F.S. Bayones, S.M. Abo-Dahab, A.M. Abd-Alla, and M.S. Soliman, "Mixed convection effect on MHD Oldroyd-B nanofluid flow over a stretching sheet through a porous medium with viscous dissipation-chemical engineering applications," Alexandria Engineering Journal, **125**, 507-525 (2025). https://doi.org/10.1016/j.aej.2025.04.056

[11] M.D. Afifi, A. Jahangiri, and M. Ameri, "Numerical and analytical investigation of Jeffrey nanofluid convective flow in magnetic field by FEM and AGM," International Journal of Thermofluids, **25**, 100999 (2024). https://doi.org/10.1016/j.ijft.2024.100999

[12] U.K. Suma, M.M. Billah, A.R. Khan, and K.E. Hoque, "Magnetohydrodynamic mixed convective heat transfer augmentation in a rectangular lid-driven enclosure with a circular hollow cylinder utilizing nanofluids," International Journal of Thermofluids, **25**, 101014 (2024). https://doi.org/10.1016/j.ijft.2024.101014

[13] Md. Irfan, T. Muhammad, M. Rashid, M.S. Anwar, S.S. Abas, and P.V.S. Narayana, "Numerical study of nonlinear thermal radiation and Joule heating on MHD bioconvection Carreau nanofluid with gyrotactic microorganisms," Journal of Radiation Research and Applied Sciences, **18**, 101254 (2024). https://doi.org/10.1016/j.jrras.2024.101254

[14] U.K. Suma, M.M Billah, and A.R. Khan, "Optimization and sensitivity analysis of unsteady MHD mixed convective heat transfer in a lid-driven cavity containing a double-pipe circular cylinder using nanofluids," International Journal of Thermofluids, **27**, 101197 (2025). https://doi.org/10.1016/j.ijft.2025.101197

[15] P. Deepalakshmi, G. Shankar, E.P. Siva, D. Tripathi, and A.O. Beg, "MHD analysis of couple stress nanofluid through a tapered non-uniform channel with porous media and slip-convective boundary effects," International Journal of Thermofluids, **27**, 101208 (2025). https://doi.org/10.1016/j.ijft.2025.101208

[16] U. Habiba, M.N. Hudha, B. Neogi, S. Islam, and M.M. Rahman, "Numerical exploration on n-decane nanofluid based MHD mixed convection in a lid driven cavity: impact of magnetic field and thermal radiation," International Journal of Thermofluids, **27**, 101209 (2025). https://doi.org/10.1016/j.ijft.2025.101209

[17] B.K. Mahatha, R. Nandkeolyar, G.K. Mahato, and P. Sibanda, "Dissipative Effects in Hydromagnetic Boundary Layer Nanofluid Flow Past A Stretching Sheet with Newtonian Heating," Journal of Applied Fluid Mechanics, **9**(4), 1977-1989 (2016). https://doi.org/10.18869/acadpub.jafm.68.235.24451

[18] R. Nandkeolyar, B.K. Mahatha, G.K. Mahato, and P. Sibanda, "Effect of Chemical Reaction and Heat Absorption on MHD Nanoliquid Flow Past a Stretching Sheet in the Presence of a Transverse Magnetic Field," Magnetochemistry, **4**(1), 1-14 (2018). https://doi.org/10.3390/magnetochemistry4010018

[19] G.K. Mahato, B.K. Mahatha, R. Nandkeolyar, and B. Patra, "The Effects of Chemical Reaction on Magnetohydrodynamic Flow and Heat transfer of a Nanofluid past a Stretchable Surface with Melting," AIP Conference Proceedings, **2253**, 020011 (2020). https://doi.org/10.1063/5.0019205

[20] G.K. Mahato, B.K. Mahatha, S. Ram, and S.B. Padhi, "Radiative and Convective Heat Transfer on MHD Stagnation point Nanofluid Flow past a Stretchable Surface with Melting," AIP Conference Proceedings, **2435**, 020037 (2022). https://doi.org/10.1063/5.0083936

[21] B.K. Mahatha, S.B. Padhi, G.K. Mahato, and S. Ram, "Radiation, Chemical Reaction and Dissipative Effects on MHD Stagnation Point Nano-Fluid Flow Past a Stretchable Melting Surface," AIP Conference Proceedings, **2435**, 020040 (2022). https://doi.org/10.1063/5.0083933

[22] R.H. Hameed, R.A. Hussein, Q.H. Al-Salami, M.A. Alomari, A.M. Hassan, F.Q.A. Alyousuf, F. Alqurashi, *et al*.," Free convection investigation for a Casson-based $Cu - H_2O$ nanofluid in semi parabolic enclosure with corrugated cylinder," Heliyon, **11**, e40960 (2024). https://doi.org/10.1016/j.heliyon.2024.e40960
[23] S. Zeb, Z. Ullah, A.B. Albidah, I, Khan, and W.A. Khan, "The significance of heat transfer through natural convection in stagnation point flow of prandtl fluid," Results in Physics, **68**, 108087 (2024). https://doi.org/10.1016/j.rinp.2024.108087
[24] M.D Afifi, A. Jahangiri, and Md. Ameri, "Investigation of natural convection heat transfer in MHD fluid within a hexagonal cavity with circular obstacles," International Journal of Thermofluids, **25**, 101024 (2024). https://doi.org/10.1016/j.ijft.2024.101024
[25] M. Saghafian, M. Moslehi, and O.A. Akbari, "Magnetohydrodynamic unsteady natural convection slip flow in a vertical parallel plate microchannel heated with constant heat flux," Heliyon, **11**, e41502 (2024). https://doi.org/10.1016/j.heliyon.2024.e41502
[26] R. Nciri, A.E.A. Awouda, A.A. Musa, H.G. Alshomrani, and F. Nasri, "Numerical Simulation of Natural Convection in a Chamfered Square Cavity with Fe_3O_4-Water Nanofluid and Magnetic Excitation," Engineering, Technology & Applied Science Research, **15**(1), 20523–20528 (2025). https://doi.org/10.48084/etasr.9775
[27] A. Ali, Rabia, S. Hussain, and M. Ashraf, "Theoretical investigation of unsteady MHD flow of Casson hybrid nanofluid in porous medium: Applications of thermal radiations and nanoparticle," Journal of Radiation Research and Applied Sciences, **17**(1), 101029 (2024). https://doi.org/10.1016/j.jrras.2024.101029
[28] Z.H. Khan, W.A. Khan, S.M. Ibrahim, K. Swain, Z. Huang, "Impact of multiple slips and thermal radiation on heat and mass transfer in MHD Maxwell hybrid nanofluid flow over porous stretching sheet," Case Studies in Thermal Engineering, **61**, 104906 (2024). https://doi.org/10.1016/j.csite.2024.104906
[29] N. Manjunatha, M.G. Reddy, A. Aloqaily, S. Aljohani, A.R. Reddy, F. Ali, and N. Mlaiki, "Radiation effects on rotating system free convective nanofluid unsteady flow with heat source and magnetic field," Partial Differential Equations in Applied Mathematics, **13**, 101083 (2025). https://doi.org/10.1016/j.padiff.2025.101083
[30] R.D. Alsemiry, S.E. Ahmed, M.R. Eid, and M.E. Essam, "ANN-Based Prediction and RSM Optimization of Radiative Heat Transfer in Couple Stress Nanofluids with Thermodiffusion Effects," Process, **13**(4), 1055 (2025). https://doi.org/10.3390/pr13041055
[31] A. Khan, Hashim, M. Farooq, W. Jamshed, B.M. Makhdoum, and N.A.A.M. Nasir, "Nonlinear convective heat transfer in Maxwell nanofluids with quadratic thermal stratification over a Magnetized inclined Surface: Applications towards engineering Industry," Ain Shams Engineering Journal, **16**, 103432 (2025). https://doi.org/10.1016/j.asej.2025.103432
[32] W. Li, S.A. Khan, M. Shafqat, Q. Abbas, T. Muhammad, and M. Imran, "Computational analysis for efficient thermal transportation of ternary hybrid nanofluid flow across a stretching sheet with Cattaneo-Christov heat flux model," Case Studies in Thermal Engineering, **66**, 105706 (2024). https://doi.org/10.1016/j.csite.2024.105706
[33] S.R. Mishra, I. Haq, R. Baithalu, S. Panda, and A. Saeed, "Transient radiative flow of hybrid nanofluid under slip effects over an impermeable spinning disk with porous material," Partial Differential Equations in Applied Mathematics, **14**, 101154 (2025). https://doi.org/10.1016/j.padiff.2025.101154
[34] S.M. Sait, A. Riaz, S. Shaheen, R. Ellahi, and S. Akram, "Thermally induced cilia flow of Prandtl nanofluid under the influence of electroosmotic effects with boundary slip," Journal of Taibah University for Science, **19**, 2484877 (2025). https://doi.org/10.1080/16583655.2025.2484877
[35] Y. Ouyang, Md. Faisal, Md. Basir, K. Naganthran, and I. Pop, "Exploring velocity slip and stability in unsteady ternary nanofluid flow past a permeable stretching/shrinking sheet," Journal of Taibah University for Science, **19**, 2487302 (2025). https://doi.org/10.1080/16583655.2025.2487302
[36] B.K. Mahatha, R. Nandkeolyar, G. Nagaraju, and M. Das, "MHD stagnation point flow of a nanofluid with velocity slip, Non-linear radiation and Newtonian heating," Procedia Engineering, **127**, 1010-1017 (2015). https://doi.org/10.1016/j.proeng.2015.11.450

ВПЛИВ ПРИРОДНОЇ КОНВЕКЦІЇ ТА ВИПРОМІНЮВАННЯ НА МГД-ТЕЧІЮ НАНОРІДИНИ В ТОЧЦІ ЗАСТОЮ, ЩО ПРОТІКАЄ ПОВЗ РОЗТЯГУВАНУ ПОВЕРХНЮ ІЗ ШВИДКІСНИМ КОВЗАННЯМ І НЬЮТОНІВСЬКИМ НАГРІВАННЯМ

Г.П. Гіфті[a], С.Б. Падхі[a], Б.К. Махатха[b], Г.К. Махато[c]
[a]*Кафедра математики, Технологічний та менеджментний університет Центуріон, Одіша, Індія*
[b]*Середня школа Раджкіякрит +2, Латбедхва, Кодерма, Джаркханд, Індія*
[c]*Кафедра математики, Інститут прикладних наук Аміті, Університет Аміті, Джаркханд, Ранчі-835303, Індія*

Досліджується природний конвекційний потік в'язкої, нестисливої, електропровідної та випромінюючої тепло нанорідини в точці застою МГД повз розтягувану поверхню з ковзанням за швидкістю та ньютонівським нагріванням у присутності поперечного магнітного поля. Розв'язуються відповідні нелінійні диференціальні рівняння в частинних похідних за допомогою методу bvp4c Matlab. Для підтвердження надійності та точності результату, числові результати цього дослідження порівнюються з існуючою літературою, і було виявлено, що вони добре узгоджуються. Вплив різних параметрів на швидкість, температуру та концентрацію речовин обчислюється та представляється у вигляді графіків, тоді як вплив тертя поверхні, швидкість теплопередачі та швидкість масопередачі зведено в таблиці. В результаті посиленого накопичення або дифузії теплової енергії температура нанорідини збільшується внаслідок броунівського руху, термофоретичної дифузії, швидкісне ковзання, конвективного нагрівання, нелінійного теплового випромінювання та числа Прандтля. Швидкість теплопередачі збільшується внаслідок співвідношення температур, конвективного нагрівання та теплового числа Грасгофа завдяки збільшенню теплових градієнтів та теплопередачі, зумовленої плавучістю. Такі потоки нанорідин мають потенціал для використання в низці процесів теплопередачі, таких як пристрої відновлюваної енергії, включаючи МГД-генератори, тощо.
Ключові слова: *МГД; нанорідина; природна конвекція; випромінювання; швидкісне ковзання; ньютонівське нагрівання*